Journal of Hazardous Materials 190 (2011) 686–693

Contents lists available at ScienceDirect

Journal of Hazardous Materials

journal homepage: www.elsevier.com/locate/jhazmat

Biological removal of nitrate by an oil reservoir culture capable of autotrophic and heterotrophic activities: Kinetic evaluation and modeling of heterotrophic process

Shijie An [a], Heather Stone [b], Mehdi Nemati [b,*]

[a] Division of Environmental Engineering, University of Saskatchewan, 57 Campus Drive, Saskatoon, Canada
[b] Department of Chemical Engineering, University of Saskatchewan, 57 Campus Drive, Saskatoon, Canada

ARTICLE INFO

Article history:
Received 24 January 2011
Received in revised form 28 March 2011
Accepted 28 March 2011
Available online 4 April 2011

Keywords:
Heterotrophic denitrification
Nitrate
Continuous bioreactor
Biokinetics
Modeling

ABSTRACT

Kinetics of heterotrophic denitrification was investigated using an oil reservoir culture with the ability to function under both autotrophic and heterotrophic conditions. In the batch system nitrate at concentrations up to 30 mM did not influence the kinetics but with 50 mM slower growth and removal rates were observed. A kinetic model, representing the denitrification as reduction of nitrate to nitrite, and subsequent reduction of nitrite to nitrous oxides and nitrogen gas was developed. The value of various kinetic coefficients, including maximum specific growth rate, saturation constant, yield and activation energy for nitrate and nitrite reductions were determined by fitting the experimental data into the developed model. In continuous bioreactors operated with 10 or 30 mM nitrate, complete removal of nitrate (no residual nitrite) and linear dependency between nitrate loading and removal rates were observed for loading rates up to 0.21 and 0.58 mM h^{-1}, respectively. The highest removal rates of 0.31 and 0.94 mM h^{-1} observed at loading rates of 0.42 mM h^{-1} and 1.26 mM h^{-1}, with corresponding removal percentages of nitrate and total nitrogen being 75.4, 54.4%, and 74.4 and 17.9%, respectively. Developed kinetic model predicted the performance of the continuous bioreactors with accuracy.

© 2011 Elsevier B.V. All rights reserved.

1. Introduction

Contamination of ground and surface waters with nitrate and ammonia is a major environmental concern. For instance release of nitrogenous compounds in water bodies could lead to eutrophication and disruption of the ecosystem in such waters [1,2]. Extensive use of fertilizers and discharge of partially treated domestic wastes contribute to contamination of surface and ground waters with nitrate. Nitrate containing wastewaters are generated in manufacturing of cellophane, explosives, fertilizers, pectin, and in metal finishing processes and could contain more than 1000 mg NO_3-N L^{-1} [5,6]. Excessive level of nitrate in some ground waters, used as the main drinking water source, has been reported [3] which could cause severe health problems such as methemoglobinemia, and potential formation of carcinogens in stomach and intestine [4]. The nitrate standards for the drinking water recommended by the World Health Organization, the United States Environmental Protection Agency, and the Council of European Communities are 11.3, 10 and 11.3 mg NO_3-N L^{-1}, respectively, and for the nitrite are 0.9, 1 and 0.03 mg NO_3-N L^{-1} [5].

Nitrate removal can be achieved by physicochemical methods such as reverse osmosis, ion exchange, catalytic conversion, and by biological processes [4,6]. Biological removal of nitrate could occur as a result of nitrate uptake by plants and microorganisms, or through biological transformation of nitrate to nitrogen, referred to as denitrification. Denitrification process which also serves as a critical step in removal of ammonia from domestic wastewaters [1] relies on the activity of denitrifying bacteria which use nitrate or nitrite as an electron acceptor during the oxidation of organic or inorganic compounds for the purpose of energy generation. Denitrification occurs through a number of sequential reactions in which nitrate is reduced to nitrite, and subsequently to nitrogen oxides and nitrogen gas, as described below [7]:

$$NO_3^- + 2e^- + 2H^+ \rightarrow NO_2^- + H_2O \quad (1)$$

$$NO_2^- + e^- + 2H^+ \rightarrow NO + H_2O \quad (2)$$

$$NO + e^- + H^+ \rightarrow 1/2N_2O + 1/2H_2O \quad (3)$$

$$1/2N_2O + e^- + H^+ \rightarrow 1/2N_2 + 1/2H_2O \quad (4)$$

Autotrophic denitrifying bacteria use sulphide, sulphur, or hydrogen as the electron donor, while heterotrophic denitrifiers utilize various organic compounds such as methanol, ethanol, formate, acetate, and lactate as electron donor [3,7,8]. Studies of

* Corresponding author. Tel.: +1 306 966 4769; fax: +1 306 966 4777.
E-mail address: Mehdi.Nemati@usask.ca (M. Nemati).

0304-3894/$ – see front matter © 2011 Elsevier B.V. All rights reserved.
doi:10.1016/j.jhazmat.2011.03.102

Nomenclature

D	dilution rate (h^{-1})
$E_{\mu\text{-}NO_3}$	activation energy, nitrate reduction (kJ mol^{-1})
$E_{\mu\text{-}NO_2}$	activation energy, nitrite reduction (kJ mol^{-1})
$K_{S\text{-}NO_3}$	saturation constant, nitrate reduction (mM NO_3)
$K_{S\text{-}NO_2}$	saturation constant, nitrite reduction (mM NO_2)
$K_{d\text{-}NO_3}$	decay coefficient, nitrate reduction (h^{-1})
$K_{d\text{-}NO_2}$	decay coefficient, nitrite reduction (h^{-1})
$S_{0\text{-}Ace}$	initial acetate concentration (mM)
S_{Ace}	acetate concentration (mM)
$S_{0\text{-}NO_3}$	initial nitrate concentration (mM)
S_{NO_3}	nitrate concentration (mM)
$S_{0\text{-}NO_2}$	initial nitrite concentration (mM)
S_{NO_2}	nitrite concentration (mM)
t	time (h)
X_0	initial biomass concentration (g L^{-1})
X	biomass concentration (g L^{-1})
$Y_{X\text{-}NO_3}$	nitrate biomass yield, g cell-dry weight (mM NO_3)$^{-1}$
$Y_{X\text{-}NO_2}$	nitrite biomass yield, g cell-dry weight (mM NO_2)$^{-1}$
$Y_{X\text{-}Ace\text{-}NO_3}$	acetate biomass yield, nitrate reduction, g cell-dry weight (mM Ace)$^{-1}$
$Y_{X\text{-}Ace\text{-}NO_2}$	acetate biomass yield, nitrite reduction, g cell-dry weight (mM Ace)$^{-1}$
$\mu_{max\text{-}NO_3}$	maximum specific growth rate, nitrate reduction (h^{-1})
$\mu_{max\text{-}NO_2}$	maximum specific growth rate, nitrite reduction (h^{-1})

heterotrophic denitrification have focused on various aspects of this process including type of the electron donor [2,9–11], kinetic modeling [3,7,12,13], bioreactor design [4,6,14–17], and simultaneous nitrification and denitrification (SND) process [1,18,19]. Autotrophic denitrification has attracted much attention in recent years due to its beneficial applications in desulphurization of sour gases, biogas, and sulphide laden waters, as well as its critical role in the in situ removal of H_2S from the oil reservoirs subjected to water flooding [8]. Various aspects of autotrophic denitrification thus have been investigated extensively [20–33]

Coleville enrichment is a mixed microbial culture originated from the produced water of a Canadian oil reservoir and possesses superior characteristics as far as biodesulphurization is concerned [23,32,33]. Specifically, *Thiomicrospira denitrificans* CVO, the main microbial component of Coleville enrichment, could tolerate and oxidize sulphide at concentrations as high as 18 mM and is capable of both autotrophic and heterotrophic activities [34]. Process of autotrophic denitrification by Coleville enrichment has been studied in our earlier work [32,33]. Results have indicated that in the presence of sufficient nitrate, sulphide is the preferred electron donor and oxidation of acetate occurs only after oxidation of sulphide to sulphur and complete exhaustion of sulphide. In the absence of sulphide, sulphur and acetate are oxidized simultaneously and oxidation of acetate proceeds much faster than that of sulphur [32,33].

Unique characteristics of Coleville enrichment such as functioning both autotrophically and heterotrophically, and tolerance of sulphide at concentrations as high as 18 mM, much higher than those reported in literature for other sulphide oxidizing strains, offer great potential for application of this enrichment in a process for simultaneous removal of sulphide, nitrate, nitrite and BOD. Utilization of Coleville enrichment in such process, however, requires a thorough understanding of the heterotrophic denitrification kinetics by this culture which currently does not exist. The objective of the present work was, therefore, to study the kinetics of heterotrophic denitrification by Coleville enrichment using batch and continuous bioreactors. A kinetic model representing the denitrification as a two-step process (reduction of nitrate to nitrite, and subsequently to nitrogen oxides and nitrogen gas) was developed. The experimental data obtained in the batch and continuous systems were used to determine the kinetics coefficients for the reductions of nitrate and nitrite. Evaluation of the developed model by an independent set of experimental data and sensitivity analysis was also performed.

2. Materials and methods

2.1. Microbial culture and medium

The heterotrophic denitrifying culture (h-NRB) used in this study was enriched from the produce water of the Coleville oil field, located in Saskatchewan, Canada. The procedure for the enrichment and maintenance of this culture has been described elsewhere [33]. Coleville Synthetic Brine (CSB) containing per liter: 7.0 g NaCl, 0.68 g $MgSO_4{\cdot}7H_2O$, 0.24 g $CaCl_2{\cdot}2H_2O$, 0.02 g NH_4Cl, 0.027 KH_2PO_4, 0.68 $NaCH_3COO{\cdot}3H_2O$, 1.0 g KNO_3, 1.9 g $NaHCO_3$, 6.06 g Tris Base and 0.5 mL trace element solution was used as medium [33]. COD to nitrate ratio in the CSB medium was maintained at 2 mM O_2 (mM NO_3)$^{-1}$ to ensure that acetate was in excess of the theoretical level required for complete reduction of nitrate to N_2 (1.25 mM O_2/mM NO_3). This is due to the fact that complete reduction of 1 mM nitrate to N_2 theoretically requires 0.625 mM acetate, and that oxidation of 1 mM acetate consumes 2 mM O_2 [7]. pH of the medium was adjusted to 7.0–7.5 using 2 M HCl. Cultures were maintained at room temperature (25 °C) and subcultured every two weeks.

2.2. Batch experiments

To study the effect of nitrate initial concentration, serum bottles (125 mL) containing 100 mL CSB medium with 30.6 ± 0.6 mM acetate and 5, 10, 15, 20, 30 or 50 mM nitrate (COD to nitrate ratios: 12, 6, 4, 3, 2 and 1.2 mM O_2 (mM NO_3)$^{-1}$, respectively) and pH of 7.0–7.5 were purged with filter sterilized nitrogen for 5 min to remove the dissolved oxygen. The bottles were sealed with rubber septum and autoclaved for 30 min at 121 °C. Bottles were then inoculated with three-day old h-NRB enrichment (10% v/v), maintained at room temperature (25 °C) and sampled regularly. Optical density, as an indication of biomass concentration, was determined in each sample immediately. The remaining portion of the sample was centrifuged for 5 min at 9180 (×g) and the supernatant was used for analysis of acetate, nitrite and nitrate. Based on the stoichiometry, concentration of acetate was in excess of the level required for complete reduction of nitrate to N_2. Effect of temperature (15, 20, 30, 35 °C) was investigated in an incubator with the desired temperature, using CSB medium containing 24.3 ± 1.9 mM acetate and 17.5 ± 0.4 nitrate (COD to nitrate ratio: 2.8 mM O_2 (mM NO_3)$^{-1}$). All other conditions and procedures were similar to those described earlier. Since all the experiments aiming to study the effect of nitrate concentration were carried out at 25 °C, this temperature was not tested again. All batch experiments were carried out in duplicates. Control runs were conducted under similar conditions without inoculation. Data generated in the batch experiments with 5, 10, 20, 30 and 50 mM nitrate at 25 °C, and those obtained with 24.3 ± 1.9 mM nitrate at 15, 20, 30, 35 °C were used to determine various kinetic coefficients, as described in section 2.4. Batch data obtained with 15 mM nitrate at 25 °C were used for validation of the kinetic model.

2.3. Continuous experiments

Heterotrophic denitrification was also studied in continuous systems (two identical set-ups). Each set-up consisted of a glass bioreactor (working volume: 230 mL) with a small stirrer and a sampling port with rubber septum, feed and effluent containers, and a peristaltic pump. CSB Medium with either 10.4 ± 0.5 mM acetate and 10.7 ± 0.5 mM nitrate (COD to nitrate ratio: 1.9 mM O_2 (mM NO_3)$^{-1}$), or 28.7 ± 1.1 mM acetate and 31.4 ± 1.0 mM nitrate (COD to nitrate ratio: 1.8 mM O_2 (mM NO_3)$^{-1}$) was prepared in a glass flask and autoclaved for 30 min at 121 °C. After cooling, medium was purged with filter sterilized nitrogen for an hour. Medium was then transferred into a sterilized collapsible medium bag by introducing pressurized sterilized nitrogen gas into the flask. Use of collapsible bag which was connected to the bioreactor by tygon tubing maintained the anaerobic conditions and allowed proper operation of the peristaltic pump. Each bioreactor was initially charged with the designated CSB medium and purged with nitrogen gas for 10 min. A three-day old Coleville h-NRB enrichment (30 mL) was then added. Concentrations of nitrate and nitrite were monitored regularly. When residual nitrate and nitrite concentrations reached a negligible level, bioreactor was switched to continuous mode by pumping CSB medium into the bioreactor using the peristaltic pump. The effluent was transferred to the effluent container through an overflow tube. Samples (1.5 mL) were taken from the bioreactors on a daily basis and analyzed for biomass, acetate, nitrate, and nitrite concentrations, and pH. Flow rate of the feed was increased stepwise until cell wash-out occurred (0.4–26.7 mL h^{-1}). At each flow rate sufficient time was given for establishment of steady state conditions. Steady state conditions were assumed when residual nitrate, acetate and biomass concentrations changed less than 5–10% for at least three days. Following this period the bioreactor was operated at the same flow rate for 3–5 additional days and daily sampling was carried out. The average value of the data obtained in over this period was then used in assessing the performance of the bioreactor. Both experimental runs were carried out at room temperature (25 °C).

2.4. Modeling of the batch and continuous systems and model validation

To develop the kinetic model it was assumed that the denitrification proceeded in two consecutive steps of nitrate reduction to nitrite (reaction (1)), followed by reduction of nitrite to other nitrogenous compounds (reactions (2)–(4)). The concentration profiles observed in the batch experiments confirmed the validity of this assumption. Since accurate measurement of the dynamic concentration for nitrogen oxides in the liquid and gas phases is not a simple task (due to reactivity and instability), reactions (2)–(4) were combined and treated as a single step. This approach which has been used by other researchers [3,7] simplified the modeling of the system. Furthermore, it was assumed that microbial growth followed the Monod kinetics, with nitrate and nitrite being the limiting substrates in steps one and two, respectively. This was also a valid assumption since acetate was provided in excess in all experiments.

Eqs. (5)–(8), respectively, represent the mass balances for microbial growth, nitrate, nitrite and acetate utilizations in a batch system.

$$\frac{dX}{dt} = \left(\frac{\mu_{\text{max-NO}_3} S_{\text{NO}_3}}{K_{S\text{-NO}_3} + S_{\text{NO}_3}} - K_{\text{d-NO}_3}\right) X + \left(\frac{\mu_{\text{max-NO}_2} S_{\text{NO}_2}}{K_{S\text{-NO}_2} + S_{\text{NO}_2}} - K_{\text{d-NO}_2}\right) X \quad (5)$$

$$\frac{dS_{\text{NO}_3}}{dt} = -\frac{1}{Y_{X\text{-NO}_3}} \left(\frac{\mu_{\text{max-NO}_3} S_{\text{NO}_3}}{K_{S\text{-NO}_3} + S_{\text{NO}_3}} - K_{\text{d-NO}_3}\right) X \quad (6)$$

$$\frac{dS_{\text{NO}_2}}{dt} = \frac{1}{Y_{X\text{-NO}_3}} \left(\frac{\mu_{\text{max-NO}_3} S_{\text{NO}_3}}{K_{S\text{-NO}_3} + S_{\text{NO}_3}} - K_{\text{d-NO}_3}\right) X - \frac{1}{Y_{X\text{-NO}_2}} \left(\frac{\mu_{\text{max-NO}_2} S_{\text{NO}_2}}{K_{S\text{-NO}_2} + S_{\text{NO}_2}} - K_{\text{d-NO}_2}\right) X \quad (7)$$

$$\frac{dS_{\text{Ace}}}{dt} = -\frac{1}{Y_{X\text{-Ace-NO}_3}} \left(\frac{\mu_{\text{max-NO}_3} S_{\text{NO}_3}}{K_{S\text{-NO}_3} + S_{\text{NO}_3}} - K_{\text{d-NO}_3}\right) X - \frac{1}{Y_{X\text{-Ace-NO}_2}} \left(\frac{\mu_{\text{max-NO}_2} S_{\text{NO}_2}}{K_{S\text{-NO}_2} + S_{\text{NO}_2}} - K_{\text{d-NO}_2}\right) X \quad (8)$$

Eqs. (5)–(8) were solved simultaneously using a 4th order Runge-Kutta method in Excel software. Value of various kinetic coefficients was determined by fitting the data generated in the experiments with 5, 10, 20, 30 and 50 mM nitrate at 25 °C, and those obtained with 24.3 ± 1.9 mM nitrate at 15, 20, 30, 35 °C into the model, and performing non-linear regression using least-squares minimization and Solver routine within Excel™ software [35]. Eq. (9) represents the objective function used in the least square minimization:

$$f = \sum_{i}^{n} (S_{i\text{-NO}_3\text{-measured}} - S_{i\text{-NO}_3\text{-predicted}})^2 + (S_{i\text{-NO}_2\text{-measured}} - S_{\text{NO}_2\text{-predicted}})^2 + (S_{i\text{-Ace-measured}} - S_{i\text{-Ace-predicted}})^2 + (S_{i\text{-}X\text{-measured}} - S_{i\text{-}X\text{-predicted}})^2 \quad (9)$$

The values of $\mu_{\text{max-NO}_3}$ and $\mu_{\text{max-NO}_2}$ obtained at different temperatures were fitted to Arrhenius expression and activation energies for growth on nitrate ($E_{\mu\text{-NO}_3}$) and nitrite ($E_{\mu\text{-NO}_2}$) were determined. Batch data obtained with 15 mM nitrate at 25 °C were used for validation of the kinetic model.

The dynamic behaviour of the continuous bioreactor was modeled using the mass balances for biomass, nitrate, nitrite and acetate, as given by expressions (10)–(13), respectively.

$$\frac{dX}{dt} = D(X_0 - X) + \frac{\mu_{\text{max-NO}_3} S_{\text{NO}_3}}{K_{S\text{-NO}_3} + S_{\text{NO}_3}} X + \frac{\mu_{\text{max-NO}_2} S_{\text{NO}_2}}{K_{S\text{-NO}_2} + S_{\text{NO}_2}} X \quad (10)$$

$$\frac{dS_{\text{NO}_3}}{dt} = D(S_{0\text{-NO}_3} - S_{\text{NO}_3}) - \frac{1}{Y_{X\text{-NO}_3}} \frac{\mu_{\text{max-NO}_3} S_{\text{NO}_3}}{K_{S\text{-NO}_3} + S_{\text{NO}_3}} X \quad (11)$$

$$\frac{dS_{\text{NO}_2}}{dt} = D(S_{0\text{-NO}_2} - S_{\text{NO}_2}) + \frac{1}{Y_{X\text{-NO}_3}} \frac{\mu_{\text{max-NO}_3} S_{\text{NO}_3}}{K_{S\text{-NO}_3} + S_{\text{NO}_3}} X - \frac{1}{Y_{X\text{-NO}_2}} \frac{\mu_{\text{max-NO}_2} S_{\text{NO}_2}}{K_{S\text{-NO}_2} + S_{\text{NO}_2}} X \quad (12)$$

$$\frac{dS_{\text{Ace}}}{dt} = D(S_{0\text{-Ace}} - S_{\text{Ace}}) - \frac{1}{Y_{X\text{-Ace-NO}_3}} \frac{\mu_{\text{max-NO}_3} S_{\text{NO}_3}}{K_{S\text{-NO}_3} + S_{\text{NO}_3}} X - \frac{1}{Y_{X\text{-Ace-NO}_2}} \frac{\mu_{\text{max-NO}_2} S_{\text{NO}_2}}{K_{S\text{-NO}_2} + S_{\text{NO}_2}} X \quad (13)$$

Considering that the value of decay coefficients determined from the batch data were small (10^{-5} to 10^{-6} h^{-1}), decay term was not included. Eqs. (10)–(13) were solved simultaneously to determine the transient concentrations of biomass, nitrate, nitrite and acetate at each dilution rate. The theoretical steady state concentrations at each dilution rate were determined by conducting the calculations in the transient model over a sufficiently long time.

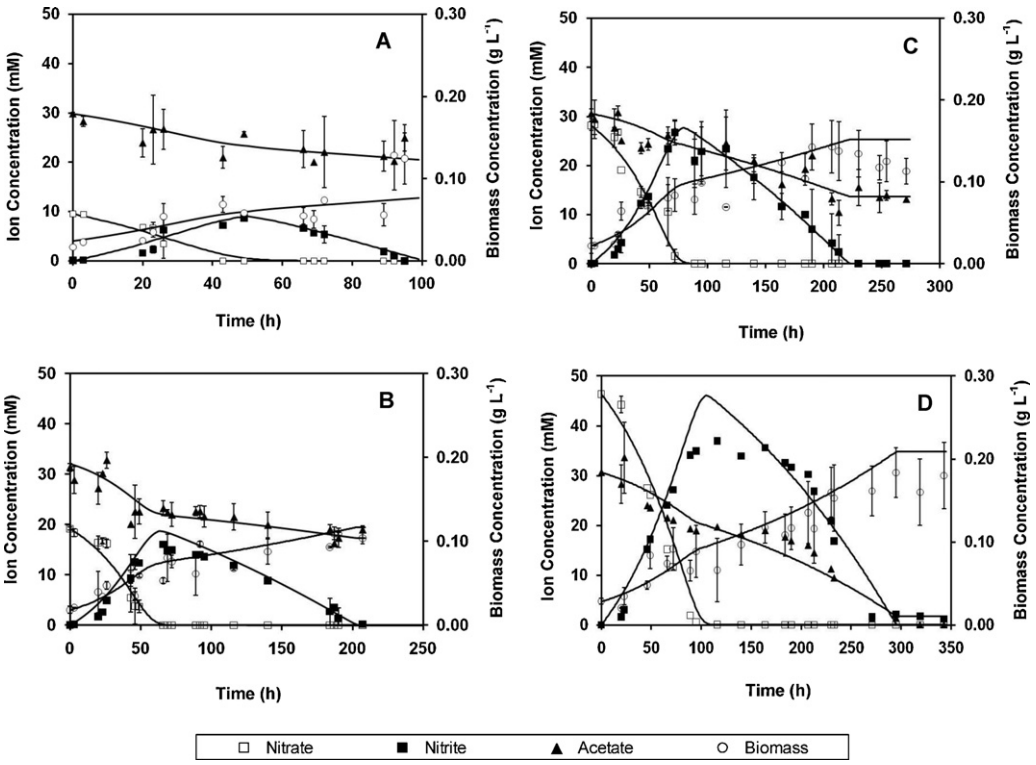

Fig. 1. Batch denitrification of 10 mM (A), 20 mM (B), 30 mM (C) and 50 mM (D) nitrate. Symbols are the average value of the data obtained in duplicate experiments and error bars are the associated standard deviations. Solid lines represent the model prediction.

Finally, the values of various kinetic coefficients were determined by fitting the steady state experimental data at each dilution rate into the model. All the calculations were performed in Excel™ software using 4th order Runge-Kutta method and least square minimization as described for the batch system.

2.5. Analytical procedures

Optical density of the samples was determined at 620 nm (SHIMADZU UVmini-1240 Spectrophotometer, Japan). A calibration curve was developed and used to convert the optical density to biomass concentration. Concentrations of acetate, nitrate, and nitrite were determined using a Dionex Ion chromatograph (ICS-2500) with a thermal conductivity detector (CD25A), an IonPac CG5A guard column and an IonPac CS5A analytical column (Dionex Corporation, Sunnyvale, CA, USA). KOH (1 mM) with a flow rate of 1.5 mL h^{-1} was used as eluent.

3. Results and discussion

3.1. Batch system

Fig. 1 shows the profiles of biomass, nitrate, nitrite and acetate concentrations in the experiments with 10, 20, 30, 50 mM nitrate at 25 °C. Results for experiments with 5 and 15 mM nitrate are not included but profiles were similar to those shown in Fig. 1. In all cases microbial activity started without any delay, resulting in removal of nitrate and formation of nitrite at similar rates. Removal of nitrite began only when nitrate concentration dropped to a low level. This pattern which occurred regardless of nitrate initial concentration was similar to that observed during the autotrophic denitrification with sulphide [32]. In other words in both cases nitrate was reduced to nitrite first and following the exhaustion of nitrate bacteria utilized nitrite as electron acceptor and reduced it to other compounds (i.e. NO, N_2O and N_2). Microbial growth and acetate utilization occurred in both steps of denitrification, albeit at faster rate during the reduction of nitrate to nitrite. Concentrations of nitrate and acetate remained unchanged and no nitrite was detected in the control experiments.

Effect of temperature on the denitrification process is shown in Fig. 2. Regardless of the applied temperature denitrification proceeded by reduction of nitrate to nitrite and subsequent reduction of produced nitrite to other gaseous end products. Increase of temperature enhanced the microbial activity and removal rates in both steps but the effect was more pronounced during the nitrite reduction. For instance nitrate and nitrite removal rates at 15 °C were 0.24 and 0.08 mM h^{-1}, respectively, while at 35 °C the removal rates of 0.71 and 0.41 mM h^{-1} were obtained.

Model predictions for biomass, nitrate, nitrite, and acetate concentrations are included in Figs. 1 and 2 as solid lines, and associated kinetic coefficients are summarized in Table 1. Evaluation of the kinetic coefficients did not imply any particular pattern as far as nitrate initial concentration was concerned, with the exception of maximum specific growth ($\mu_{max\text{-}NO_3}$) which was 46% smaller than the mean value when 50 mM nitrate was used. Increase of temperature in the range 15–35 °C increased the value of ($\mu_{max\text{-}NO_3}$) and $\mu_{max\text{-}NO_2}$ by almost 4 and 9 folds, respectively but did not affect the other coefficients. Using the values of $\mu_{max\text{-}NO_3}$ and $\mu_{max\text{-}NO_2}$ obtained at different temperatures and Arrhenius expression, activation energies for growth on nitrate and nitrite were determined as 48.9 and 70.5 kJ mol^{-1}, respectively (regression coefficient: 0.98 in both cases). Temperature effect was more pronounced on nitrite reduction as reflected by a sharper increase of $\mu_{max\text{-}NO_2}$ and higher activation energy.

The data generated in duplicate experiments with 15 mM nitrate at 25 °C were used to evaluate the kinetic model. Theoretical biomass, nitrate, nitrite and acetate concentrations were calculated using the average values of various coefficients (last column, Table 1), with exception of $\mu_{max\text{-}NO_3}$ and $\mu_{max\text{-}NO_2}$ for which the values obtained at 25 °C (0.031 and 0.003 h^{-1}, respectively) were

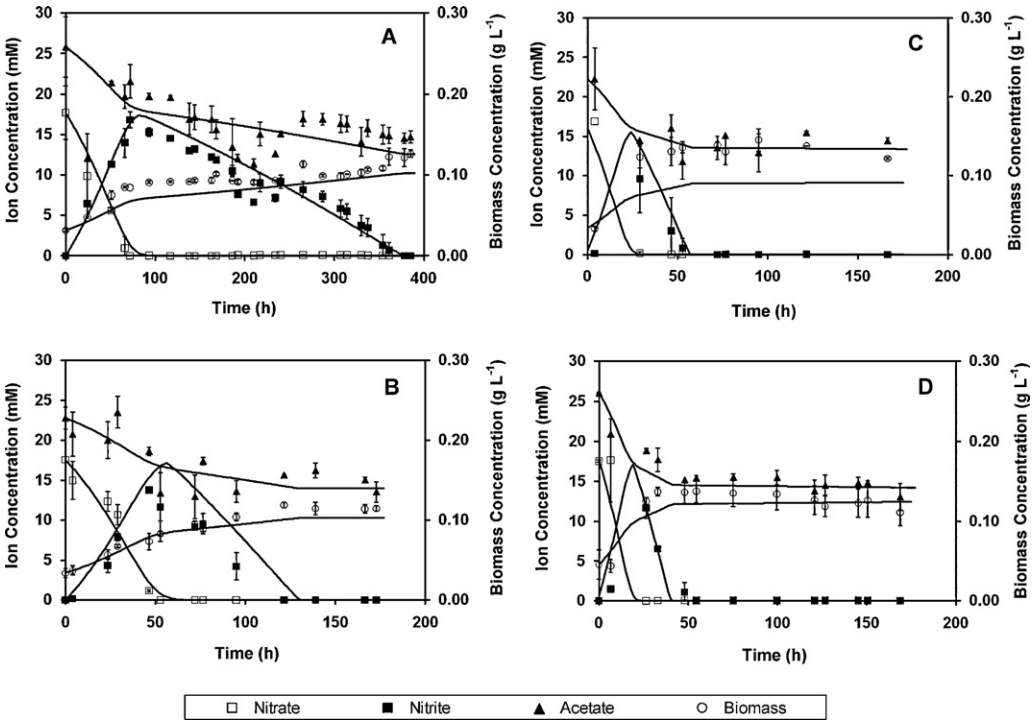

Fig. 2. Batch denitrification at 15 °C (A), 20 °C (B), 30 °C (C) and 35 °C (D). Symbols are the average value of the data obtained in duplicate experiments and error bars are the associated standard deviations. Solid lines represent the model prediction.

used. The experimental data and model predictions (solid lines) are compared in Fig. 3. The average percentage of error, calculated using the measured and predicted concentrations were 40.8%, 6.6%, 34.5% and 10.1% for biomass, nitrate, nitrite and acetate, respectively, indicating that the model predicted the experimental results with reasonable accuracy.

Sensitivity analysis was also performed by varying a particular coefficient by 10% intervals, while maintaining the others constant. The sum of square deviations (SSD) based on the measured and predicted concentrations of biomass, nitrate, nitrite and acetate was calculated for each varied parameter. Normalized sum of the squared deviations (NSSD) was defined as the ratio of SSD calculated with varied parameter to SSD calculated with the best fit parameters. A typical set of results for batch denitrification of 30 mM nitrate are shown in Fig. 4 (top panels). Maximum specific growth rates, specially $\mu_{max\text{-}NO_3}$, influenced the model prediction strongly. For instance 50% decrease in values of $\mu_{max\text{-}NO_3}$ and $\mu_{max\text{-}NO_2}$ increased the NSSD by 15 and 5 folds, respectively. Model prediction was also sensitive to yield coefficients but to a lesser extent. Variation in saturation constants did not affect the theoretical predictions significantly and the highest increase in NSSD was around 16%.

A comparison of the current results with those obtained in our earlier work on biodesulphurization (autotrophic denitrification) revealed that under both heterotrophic and autotrophic conditions, denitrification occurred through reduction of nitrate to nitrite, followed by reduction of the produced nitrite to other nitrogenous compounds. Under autotrophic conditions strong inhibitory effect of sulphide at concentrations above 18 mM limited the level of nitrate which could be removed to10 mM, due to coupling of denitrification and biodesulphurization [32]. This was not the case with heterotrophic process and nitrates at all tested concentrations (up to 50 mM) were removed effectively by the bacteria. The model developed in the present work is capable of predicting the denitrification process for nitrate concentration as high as 50 mM, a level well above that in conventional wastewaters (10–50 mg L^{-1} or 0.7–3.6 mM) and close to the level in many industrial wastewaters.

Table 1
Biokinetic coefficients based on the batch experiments data.

Nitrate Concentration (mM)	5	10	20	30	50	20				Average ± one standard deviation
Temperature (°C)	25					15	20	30	35	
$\mu_{max\text{-}NO_3}(h^{-1})$	0.031	0.029	0.031	0.024	0.014	0.014	0.024	0.043	0.054	0.014 – 0.054*
$K_{S\text{-}NO_3}(mM\ NO_3)$	2.400	2.200	2.609	2.738	2.900	2.400	2.700	2.220	2.298	2.507 ± 0.238
$K_{d\text{-}NO_3}(h^{-1})$	4.2×10^{-6}	3.5×10^{-6}	2.8×10^{-6}	4.9×10^{-6}	3.0×10^{-6}	6.1×10^{-6}	2.2×10^{-6}	7.5×10^{-6}	4.4×10^{-6}	$4.2\times10^{-6}\pm1.7\times10^{-6}$
$Y_{X\text{-}NO_3}(g\ cell\ (mM\ NO_3)^{-1})$	0.003	0.004	0.003	0.003	0.001	0.002	0.003	0.003	0.003	0.003 ± 0.001
$Y_{X\text{-}Ace\text{-}NO_3}(g\ cell\ (mM\ Ace)^{-1})$	0.001	0.006	0.006	0.012	0.006	0.005	0.008	0.006	0.006	0.006 ± 0.003
$\mu_{max\text{-}NO_2}(h^{-1})$	0.005	0.005	0.003	0.003	0.004	0.001	0.003	0.006	0.009	0.001-0.009*
$K_{S\text{-}NO_2}(mM\ NO_2)$	0.090	0.090	0.090	0.110	0.110	0.095	0.110	0.090	0.110	0.098 ± 0.010
$K_{d\text{-}NO_2}(h^{-1})$	1.4×10^{-5}	1.1×10^{-5}	1.5×10^{-5}	1.8×10^{-5}	3.5×10^{-5}	3.1×10^{-5}	5.6×10^{-6}	2.5×10^{-5}	1.2×10^{-5}	$1.8\times10^{-5}\pm9.3\times10^{-6}$
$Y_{X\text{-}NO_2}(g\ cell\ (mM\ NO_2)^{-1})$	0.001	0.002	0.002	0.002	0.002	0.002	0.001	0.001	0.001	0.002 ± 0.001
$Y_{X\text{-}Ace\text{-}NO_2}(g\ cell\ (mM\ Ace)^{-1})$	0.005	0.006	0.009	0.005	0.006	0.006	0.007	0.007	0.009	0.007 ± 0.002

* For $\mu_{max\text{-}NO_3}$ and $\mu_{max\text{-}NO_2}$, range of values observed over the tested temperatures are given.

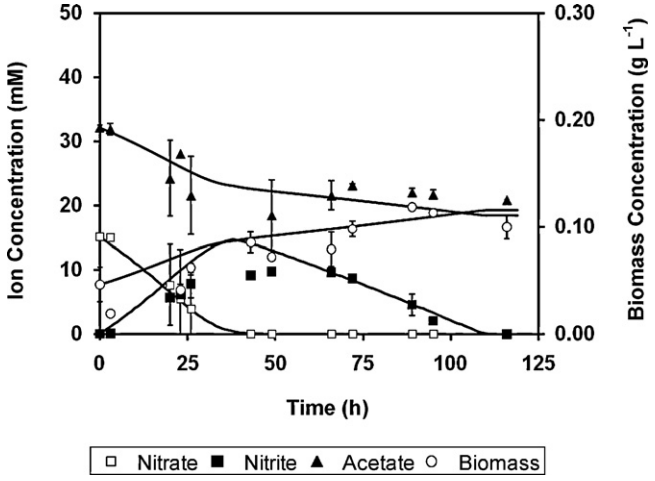

Fig. 3. Evaluation of the kinetic model with an independent set of data. Symbols are the average value of the data obtained in duplicate experiments with 15 mM nitrate at 25 °C and error bars are the associated standard deviations. Solid lines represent the model prediction.

Ersever et al. [7] studied heterotrophic denitrification by a culture from a wastewater treatment plant. Increase of temperature in the range 10–35 °C enhanced the batch denitrification kinetics, with the estimated activation energy being 59.6 kJ mol^{-1}. Batch denitrification of 7.6 mM nitrate with hydrogen as electron donor was studied by Vasiliadou et al. [3] using sludge from a wastewater treatment plant. Monod, Andrew and dual substrate (nitrate and nitrite) models were evaluated. Assumption of a two-step process similar to that in the present work, and the use of dual substrate expression resulted in the best match between the theoretical predictions and experimental data, with the value of kinetics coefficients being: $\mu_{max\text{-}NO_3} = 0.0485\,h^{-1}$, $K_{S\text{-}NO_3} = 2.05$ mM, $Y_{X\text{-}NO_3} = 0.0058$ mg biomass (mM NO_3)$^{-1}$, $\mu_{max\text{-}NO_2} = 0.55\,h^{-1}$, $K_{S\text{-}NO_2} = 0.33$ mM NO_2, and $Y_{X\text{-}NO_2} = 0.0012$ mg biomass (mM NO_2)$^{-1}$.

3.2. Continuous bioreactors

Profiles of biomass, nitrate, nitrite and acetate concentrations as a function dilution rate for continuous bioreactors are shown in Fig. 5. In both bioreactors for dilution rates up to 0.02 h^{-1} nitrate was removed completely and no residual nitrite was detected. Further increase in dilution rates led to continuous increases in residual nitrate concentration until cell wash out occurred (critical dilution rate: 0.08 h^{-1}). Nitrite concentration passed through a maximum at dilution rates around 0.03–0.04 h^{-1} and then decreased. The highest biomass concentration in the bioreactors operated with 10 and 30 mM nitrate was observed at dilution rates of 0.003 and 0.018 h^{-1}, respectively and decreased continuously as dilution rate was increased. Utilization of acetate was coupled to denitrification and as expected residual acetate concentration increased with increase of dilution rate. It is noteworthy to indicate that for the entire range of tested dilution rates, even when both nitrate and nitrite residual concentrations were zero, acetate was present in the bioreactor confirming that acetate was not a limiting substrate.

Model predictions for continuous bioreactors are included as solid lines in Fig. 5 and kinetic coefficients are summarized in Table 2. Similar to what observed in the batch system, feed nitrate concentration did not affect the denitrification kinetics and kinetic coefficients determined for 10 and 30 mM nitrate were close, as confirmed by small values of standard deviations (Table 2). When compared with the coefficients obtained for the batch system, values of maximum specific growth rates and yields were higher for the continuous system. The reason for the observed differences could lie in the fact that in a continuous system cells are not exposed to adverse conditions such as nutrient limitation, high concentra-

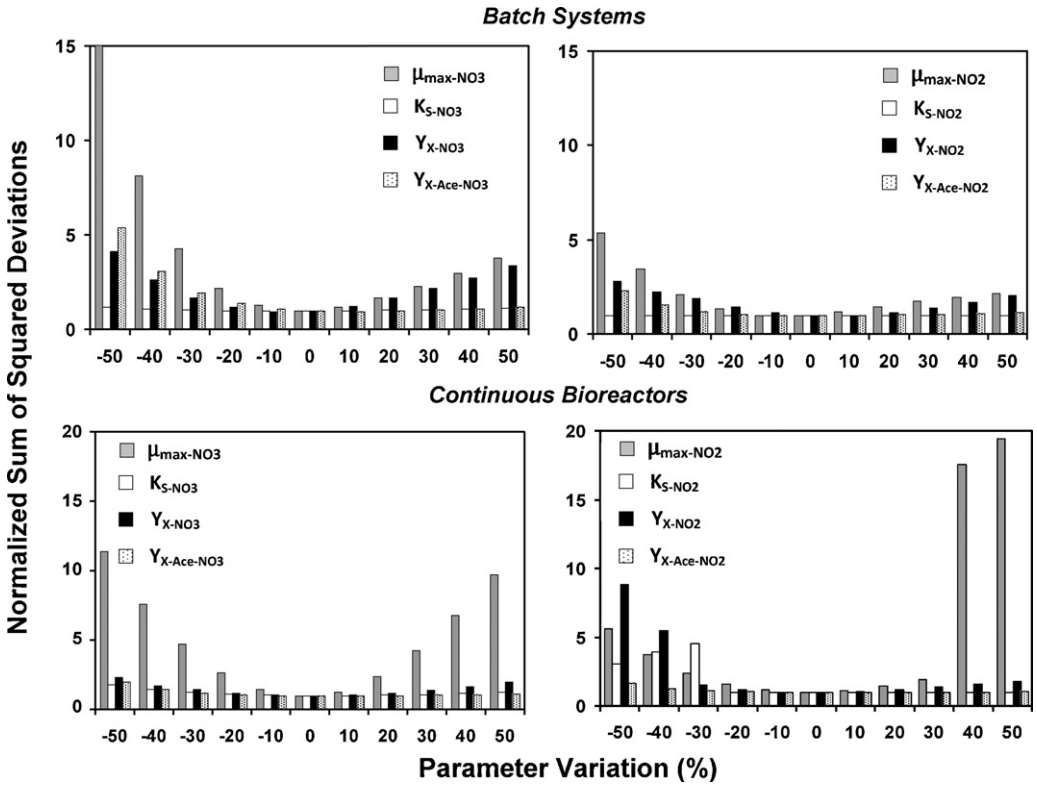

Fig. 4. Results of sensitivity analysis of the kinetic model for batch (top panels) and continuous (bottom panels) bioreactors (nitrate concentration: 30 mM; *T*: 25 °C).

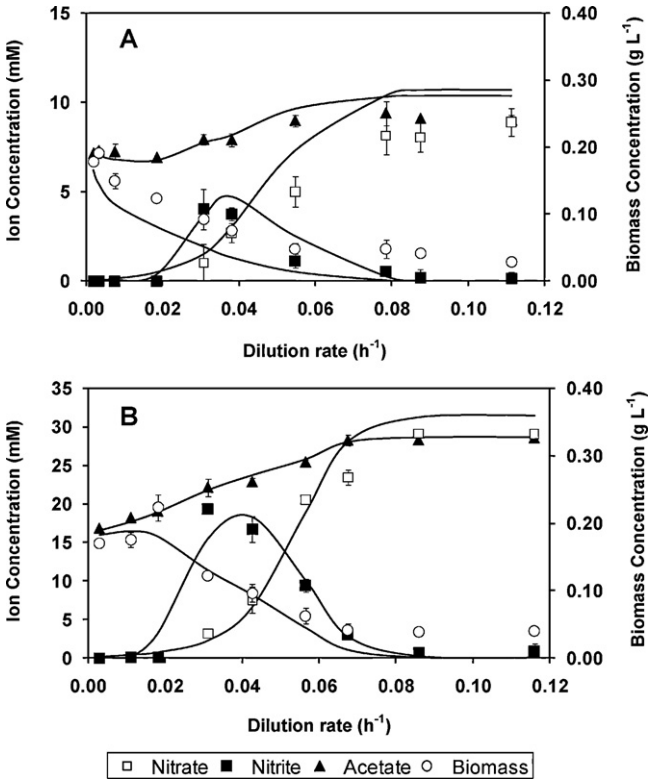

Fig. 5. Denitrification results in the continuous bioreactors operated with 10 mM (A) and 30 mM (B) of each nitrate and acetate. Symbols are the average value of the data obtained in three consecutive days after the establishment of steady state at each dilution rate and error bars are the associated standard deviations. Solid lines represent model predictions.

tions of inhibitory intermediates, and undesirable environmental pH or redox potential which may exist in a batch system [36]. Thus higher levels of metabolic activity could be expressed by cells [36]. The results of the sensitivity analyses for the continuous bioreactors are included in Fig. 4 (bottom panels). Consistent with the response observed in the batch system, maximum specific growth rates, both $\mu_{\max\text{-}NO_3}$ and $\mu_{\max\text{-}NO_2}$, strongly influenced the model predictions, while variation is saturation constants did not have a significant impact. Sensitivity to yield coefficients was also apparent but not to the extent observed with maximum specific growth rates.

Using ethanol, Ersever et al. [7] evaluated heterotrophic denitrification of either 5.4 mM nitrate or 8.5 mM nitrite in continuous bioreactors. The critical dilution rates for nitrate and nitrite operated bioreactors were 0.47 and 0.67 h^{-1}, respectively. Using Monod expression, the best fit kinetics parameters were reported as: $\mu_{\max\text{-}NO_3} = 0.75\,h^{-1}$, $K_{S\text{-}NO_3} = 0.13$ mM, $Y_{X\text{-}NO_3} = 0.0053$ mg biomass $(mM\,NO_3)^{-1}$, $Y_{X\text{-Ethanol}} = 0.0133$ mg biomass $(mM\,ethanol)^{-1}$; and $\mu_{\max\text{-}NO_2} = 0.6\,h^{-1}$, $K_{S\text{-}NO_2} = 0.62$ mM NO_2, $Y_{X\text{-}NO_2} = 0.0045$ mg biomass $(mM\,NO_2)^{-1}$ and $Y_{X\text{-Ethanol}} = 0.0133$ mg biomass $(mM\,ethanol)^{-1}$. With the exception of maximum specific growth rates, the kinetic coefficients determined in the present work are in agreement with those reported in literature for batch and continuous systems. The differences in experimental conditions such as concentration of nitrate, type of electron donor and most importantly the origin of microbial cultures are the factors which could have contributed to observed differences.

Table 2
Biokinetic coefficients based on the data from the continuous bioreactors.

Nitrate concentration (mM)	10	30	Average ± one standard deviation
$\mu_{\max\text{-}NO_3}$ (h^{-1})	0.047	0.046	0.046 ± 0.001
$K_{S\text{-}NO_3}$ $(mM\,NO_3)$	2.899	2.899	2.899 ± 0.000
$Y_{X\text{-}NO_3}$ $(g\ cell\ (mM\,NO_3)^{-1})$	0.003	0.003	0.003 ± 0.000
$Y_{X\text{-Ace-}NO_3}$ $(g\ cell\ (mM\,Ace)^{-1})$	0.019	0.019	0.019 ± 0.000
$\mu_{\max\text{-}NO_2}$ (h^{-1})	0.012	0.009	0.011 ± 0.002
$K_{S\text{-}NO_2}$ $(mM\,NO_2)$	0.110	0.085	0.097 ± 0.018
$Y_{X\text{-}NO_2}$ $(g\ cell\ (mM\,NO_2)^{-1})$	0.004	0.003	0.004 ± 0.000
$Y_{X\text{-Ace-}NO_2}$ $(g\ cell\ (mM\,Ace)^{-1})$	0.019	0.019	0.019 ± 0.000

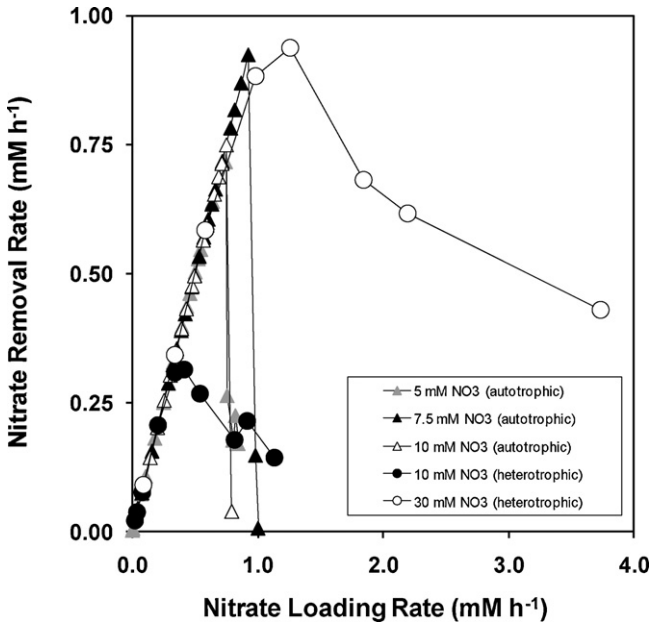

Fig. 6. Removal rate of nitrate as a function of its loading rate in the continuous bioreactors operated under heterotrophic conditions (feed: 10 mM or 30 mM of each nitrate and acetate) and autotrophic conditions (feed: 5 and 10, or 7.5 and 15, or 10 and 20 mM of nitrate and sulphide; An et al. 2010).

Fig. 6 shows the removal rate of nitrate as a function of its loading rate in the bioreactors operated with 10 and 30 mM nitrate (bioreactors 1 and 2, respectively). In bioreactor 1, complete removal of nitrate (no residual nitrite) and linear dependency between nitrate loading and removal rates were observed for loading rates up to 0.21 mM h^{-1}. In bioreactor 2 similar results obtained for loading rates as high as 0.58 mM h^{-1}. Application of loading rates higher than 0.21 and 0.58 mM h^{-1} in bioreactors 1 and 2, respectively led to accumulation of both nitrate and nitrite. In bioreactor 1, the highest removal rate of nitrate (0.31 mM h^{-1}) was obtained at a loading rate of 0.42 mM h^{-1}, with the corresponding removal percentages of nitrate and total nitrogen being 75.4 and 54.4%, respectively. The highest nitrate removal rate in bioreactor 2 was 0.94 mM h^{-1} and obtained at a loading rate of 1.26 mM h^{-1}. The removal percentages of nitrate and total nitrogen were 74.4 and 17.9%, respectively. Results of our earlier work on autotrophic denitrification with Coleville enrichment (biodesulphurization) [32] are also included in Fig. 6. As seen prior to cell wash-out linear dependency between nitrate loading and removal rates is observed under both autotrophic and heterotrophic conditions and nitrate removal rates are close (data fall on the same trend line). There are, however, two noteworthy distinctions: (1)—under autotrophic conditions cell wash out was drastic and application of loading rates slightly above a critical value caused a sudden decrease in removal rate of nitrate, while under heterotrophic conditions the observed response was less drastic. The sudden wash out observed in the autotrophic system could be attributed to the strong inhibitory effect of sulphide which at high loading rates could have hindered

the microbial activity and caused the deterioration of the bioreactor performance; (2)—under autotrophic conditions for the entire range of applied loading rates (up to 0.93 mM h^{-1}), the removal of nitrate was complete and no residual nitrite was observed in the bioreactor, while under heterotrophic conditions nitrite accumulation occurred when loading rates were above 0.21 and 0.58 mM h^{-1} in the bioreactors operated with 10 and 30 mM nitrate, respectively. The reason for the observed response is not clear. However, the results of our earlier studies [32,33] indicated that when both sulphide and acetate were present, sulphide was the preferred electron donor. Thus one could speculate that the denitrification under autotrophic conditions is the preferred pathway and led to efficient removal of both nitrate and nitrite.

4. Conclusions

Results of the present study reveal that Coleville enrichment possesses superior characteristics as far as biodesulphurization (autotrophic denitrification) and heterotrophic denitrification are concerned, and could be used in a process aiming at simultaneous removal of sulphide, nitrate, nitrite and BOD. Under autotrophic conditions the highest concentration of treated nitrate and extent of denitrification are limited by inhibitory effects of sulphide, while such limitation does not exist for heterotrophic denitrification. Furthermore, application of residence times shorter than a critical value causes sudden deterioration of autotrophic denitrification but under heterotrophic condition this effect is not as pronounced. Nitrate removal rates obtained under autotrophic and heterotrophic conditions are comparable. Under autotrophic conditions for the entire range of applied loading rates (up to 0.93 mM h^{-1}), nitrate is removed completely and no residual nitrite is observed, while under heterotrophic conditions accumulation of nitrite occurs at loading rates above 0.21 and 0.58 mM h^{-1} in bioreactors operated with 10 and 30 mM nitrate, respectively. The developed kinetic model predicts the experimental results with good accuracy and could be used in design, control and modeling of large scale systems aiming at simultaneous removal of sulphide, nitrate, nitrite and BOD.

Acknowledgements

This work was supported by a Discovery Grants from the Natural Sciences and Engineering Research Council of Canada (NSERC). Provision of a New Opportunity Fund by Canada Foundation for Innovation (CFI) is gratefully acknowledged.

References

[1] M. Morita, H. Uemoto, A. Watanabe, Nitrogen-removal bioreactor capable of simultaneous nitrification and denitrification for application to industrial wastewater treatment, Biochem. Eng. J. 41 (2008) 59–66.
[2] Y. Fernández-Nava, E. Marañón, J. Soons, L. Castrillón, Denitrification of high nitrate concentration wastewater using alternative carbon source, J. Hazard. Mater. 173 (2010) 682–688.
[3] I.A. Vasiliadou, S. Pavlou, D.V. Vayenas, A kinetic study of hydrogenotrophic denitrification, Process Biochem. 41 (2006) 1401–1408.
[4] Q. Wang, C. Feng, Y. Zhao, C. Hao, Denitrification of nitrate contaminated groundwater with a fiber-based biofilm reactor, Bioresour. Technol. 100 (2009) 2223–2227.
[5] K.A. Karanasios, I.A. Vasiliadou, S. Pavlou, D.V. Vayenas, Hydrogenotrophic denitrification of potable water: a review, J. Hazard. Mater. 180 (2010) 20–37.
[6] Y. Fernández-Nava, E. Marañón, J. Soons, L. Castrillón, Denitrification of wastewater containing high nitrate and calcium concentrations, Bioresour. Technol. 99 (2008) 7976–7981.
[7] I. Ersever, V. Ravindran, M. Pirbazari, Biological denitrification of reverse osmosis brine concentrates: I. Batch reactor and chemostat studies, Environ. Eng. Sci. 6 (2007) 503–518.
[8] K. Tang, V. Baskaran, M. Nemati, Bacteria of the sulphur cycle: an overview of microbiology, biokinetics and their role in petroleum and mining industries, Biochem. Eng. J. 44 (2009) 73–94.
[9] Y. Mokhayeri, R. Riffat, I. Takacs, P. Dold, C. Bott, J. Hinojosa, W. Bailey, S. Murthy, Characterizing denitrification kinetics at cold temperature using various carbon sources in lab-scale sequencing batch reactors, Water Sci. Technol. 58 (2008) 233–238.
[10] H.J. Choi, S.M. Lee, C.H. Choi, M.C. Kwon, H.Y. Lee, Influence of wastewater composition on denitrification and biological P-removal in the S-DN-P process: (b) effect of acetate, J. Hazard. Mater. 158 (2008) 151–156.
[11] H.J. Choi, C.H. Choi, S.M. Lee, D. Tiwari, Influence of wastewater composition on denitrification and biological P-removal in the S-DN-P process: (c) dissolved and undissolved substrates, J. Environ. Sci. 21 (2009) 1074–1079.
[12] E. Ficara, R. Canziani, Monitoring denitrification by pH-stat titration, Biotechnol. Bioeng. 98 (2007) 368–377.
[13] O. Soto, E. Aspé, M. Roeckel, Kinetics of cross-inhibited denitrification of a high load wastewater, Enzyme Microb. Technol. 40 (2007) 1627–1634.
[14] A. Rezaee, H. Godini, S. Dehestani, A.R. Yazdanbakhsh, G. Mosavi, A. Kazeminejad, Biological denitrification by *Pseudomonas stutzeri* immobilized on microbial cellulose, World J. Microbiol. Biotechnol. 24 (2008) 2397–2402.
[15] Z. Fu, F. Yang, Y. An, Y. Xue, Characteristics of nitrite and nitrate in situ denitrification in landfill bioreactors, Bioresour. Technol. 100 (2009) 3012–3015.
[16] T. Pravanova-Mancheva, V. Beschkov, Microbial denitrification by immobilized bacteria *Pseudomonas denitrificans* stimulated by constant electric field, Biochem. Eng. J. 44 (2009) 208–213.
[17] J. Shen, R. He, W. Han, X. Sun, J. Li, L. Wang, Biological denitrification of high-nitrate wastewater in a modified anoxic/oxic-membrane bioreactor (A/O-MBR), J. Hazard. Mater. 172 (2009) 595–600.
[18] G. Yilmaz, R. Lemaire, J. Keller, Z. Yuan, Simultaneous nitrification, denitrification, and phosphorus removal from nutrient-rich industrial wastewater using granular sludge, Biotech. Bioeng. 100 (2008) 529–541.
[19] E. Walters, A. Hille, M. He, C. Ochmann, H. Horn, Simultaneous nitrification/denitrification in a biofilm airlift suspension (BAS) reactor with biodegradable carrier material, Water Res. 43 (2009) 4461–4468.
[20] J. Reyes-Avila, E. Razo-Flores, J. Gomez, Simultaneous biological removal of nitrogen, carbon and sulfur by denitrification, Water Res. 38 (2004) 3313–3321.
[21] E. Vaiopoulou, P. Melidis, A. Aivasidis, Sulfide removal in wastewater from petrochemical industries by autotrophic denitrification, Water Res. 39 (2005) 4101–4109.
[22] R. Beristain-Cardoso, R. Sierra-Alvarez, P. Rowlette, E.R. Flores, J. Gomez, J.A. Field, Sulfide oxidation under chemolithoautotrophic denitrifying conditions, Biotechnol. Bioeng. 95 (2006) 1148–1157.
[23] S. Gadekar, M. Nemati, G.A. Hill, Batch and continuous biooxidation of sulphide by *Thiomicrospira* sp. CVO: reaction kinetics and stoichiometry, Water Res. 40 (2006) 2436–2446.
[24] Q. Mahmood, P. Zheng, J. Cai, D. Wu, B. Hu, J. Li, Anoxic sulphide biooxidation using nitrite as electron acceptor, J. Hazard. Mater. 147 (2007) 249–256.
[25] R. Sierra-Alvarez, R. Beristain-Cardoso, M. Salazar, J. Gómez, E. Razo-Flores, J.A. Field, Chemolithotrophic denitrification with elemental sulfur for groundwater treatment, Water Res. 41 (2007) 1253–1262.
[26] R. Beristain-Cardoso, A.C. Texier, R. Sierra-Alvarez, J.A. Field, E. Razo-Flores, J. Gómez, Simultaneous sulphide and acetate oxidation under denitrifying conditions using an inverse fluidized bed reactor, J. Chem. Technol. Biotechnol. 83 (2008) 1197–1203.
[27] C. Chen, A. Wang, N. Ren, H. Kan, D.J. Lee, Biological breakdown of denitrifying sulphide removal process in high-rate expanded granular bed reactor, Appl. Microbiol. Biotechnol. 81 (2008) 765–770.
[28] C. Jing, Z. Ping, Q. Mahmood, Effect of sulphide to nitrate ratios on the simultaneous anaerobic sulfide and nitrate removal, Bioresour. Technol. 99 (2008) 5520–5527.
[29] C. Chen, A. Wang, N. Ren, D.J. Lee, J.Y. Lai, High-rate denitrifying sulfide removal process in expanded granular sludge bed reactor, Bioresour. Technol. 100 (2009) 2316–2319.
[30] B. De Gusseme, P. De Schryver, M. De Cooman1, K. Verbeken, P. Boeckx, W. Verstraete, N. Boon, Nitrate-reducing, sulfide-oxidizing bacteria as microbial oxidants for rapid biological sulfide removal, FEMS Microbiol. Ecol. 67 (2009) 151–161.
[31] C. Jing, Z. Ping, Q. Mahmood, Simultaneous sulfide and nitrate removal in anaerobic reactor under shock loading, Bioresour. Technol. 100 (2009) 3010–3014.
[32] S. An, K. Tang, M. Nemati, Simultaneous biodesulphurization and denitrification using an oil reservoir microbial culture: Effects of sulphide loading rate and sulphide to nitrate loading ratio, Water Res. 44 (2010) 1531–1541.
[33] K. Tang, S. An, M. Nemati, M., Evaluation of autotrophic and heterotrophic processes in biofilm reactors used for removal of sulphide, nitrate and COD, Bioresour. Technol. 101 (2010) 8109–8118.
[34] D. Gevertz, A.J. Telang, G. Voordouw, G.E. Jenneman, Isolation and characterization of strains CVO and FWKO B, Two novel nitrate-reducing, sulfide-oxidizing bacteria isolated from oil field brine, Appl. Environ. Microbiol. 66 (2000) 2491–2501.
[35] H. Nikakhtari, P. Kumar, M. Nemati, G.A. Hill, Biodegradation of diesel oil in a baffled roller bioreactor, J. Chem. Technol. Biotechnol. 84 (2009) 525–532.
[36] M.L. Shuler, F. Kargi, Bioprocess engineering, in: Basic Concepts, 2nd ed., Prentice Hall PTR, Upper Saddle River, 2002.